Food Chemistry: X 15 (2022) 100425

Contents lists available at ScienceDirect

Food Chemistry: X

journal homepage: www.sciencedirect.com/journal/food-chemistry-x

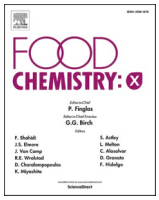

Influence of heat processing on the anti-inflammatory activity of fresh *Smilax glabra* based on PDE4 inhibition

Youjiao Wu [a], Lili He [a,c], Yi Yang [a], Zhigang Yan [c], Zhifeng Zhang [a,b], Xiaojun Yao [a], Pei Luo [a,*]

[a] *State Key Laboratories for Quality Research in Chinese Medicines, Faculty of Chinese Medicine, Macau University of Science and Technology, Macau 853, China*
[b] *Institute of Qinghai-Tibetan Plateau, Southwest Minzu University, Chengdu 610041, Sichuan Province, China*
[c] *National Engineering Institute for the Research and Development of Endangered Medicinal Resources in Southwest China, Guangxi Botanical Garden of Medicinal Plants, Nanning 530023, Guangxi Province, China*

ARTICLE INFO

Keywords:
Smilax glabra
Fresh herb
Heat processing
Anti-inflammatory activity
PDE4

ABSTRACT

Smilax glabra Roxb. (SG) is widely used as functional food with various beneficial effects. Fresh SG without processing has been eaten directly for anti-inflammation from ancient China, while the underlying mechanism remains underexplored. This study aims to investigate the anti-inflammatory activity of fresh SG by using metabolites profiles, affinity ultrafiltration mass spectrometry, PDE4 enzyme inhibition assay, and *in silico* analysis. Encouragingly, fresh SG showed promising anti-inflammatory effect with IC_{50} value (0.009 μg/μL) on PDE4 was about 12 times higher than that of processed SG (0.110 μg/μL). Astilbin was identified as the main bioactive compound of fresh SG responsible for PDE4 inhibitory activity. We found that heat processing strongly affected astilbin isomerization, leading to significant changes in contents and PDE4 inhibitory activities of four astilbin isomers, resulting in decreased anti-inflammatory activity of fresh SG. This finding will provide theoretical basis for systematic research and food/nutraceutical applications of fresh *Smilax glabra* in the future.

Introduction

Smilax glabra Roxb. (SG) (named '*Tu fuling*' in Chinese), is a rhizome of the *Liliaceae* plant, has been widely used as functional food and herbal medicine in Southeast Asia, including China, India, Vietnam, and Thailand (Hua et al., 2018). The edible plant is highly appreciated for its nutrition and health-promoting properties, especially due to the abundance of functional ingredients including bioactive flavonoids, organic acids and phenolic acids (Shu et al., 2018). Increasing evidence showed that the consumption of SG was associated with anti-inflammatory (Jiang & Xu, 2003), antioxidant (Q.-F. Zhang et al., 2009), antibacterial (Xu et al., 2013), and hepatoprotective (Thabrew et al., 2005), *etc*.

In China, fresh SG (FSG) without heat processing has a unique nutritional value and been used to treat inflammatory diseases for a long history. Originally recorded in the Tao Hongjing's *Ben Cao Jing Ji Zhu*, in which SG was called '*Yu Yu*' grain and during famine it could be eaten directly as nutritious food. The unique properties of FSG were commended in the Ming dynasty, Li Shizhen stated in *Ben Cao Gang Mu*, the illustrious medical herbal book, that SG is non-toxic, sweet, can be eaten directly without processing, which could cure syphilitic and eczema. Nowadays, FSG is still commonly available in the fresh food and herbal markets of South China, and is often used as edible or topical forms such as fruit juice, functional food and folk remedy with health function of clearing damp-heat, detoxication, easing joint movement and treating inflammation. Despite these health benefits, to our knowledge, there is no report explored the chemical compositions and biological properties of FSG, thereby, the beneficial effects and market potential for it have not been well-exploited.

In addition to the above-noted FSG, decocting with water after processing is another common form recorded in the ancient books and pharmacopoeias. Generally, drying-heating is the most applied method for processed SG (PSG), which can extend the shelf-life, prevent attacks by insects and maintain preference habits, *etc*. Therefore, before consumption, SG is commonly subjected to several different steps (washing, cutting, drying, and boiling), thus, the processing procedures for SG must at least include removing water at a certain temperature, extracting with hot water, followed by concentrating the decoction. As a result, from fresh materials to concentrated extracts, with high temperature, prolonged contact with air, pH and water, *etc.*, the contents and structures of active components may change, then alter the biological

* Corresponding author.
E-mail addresses: wuyoujiaojiao@163.com (Y. Wu), lily80s@126.com (L. He), 441214434@qq.com (Y. Yang), 287316886@qq.com (Z. Yan), zfzhang@must.edu.mo (Z. Zhang), xjyao@must.edu.mo (X. Yao), pluo@must.edu.mo (P. Luo).

https://doi.org/10.1016/j.fochx.2022.100425
Received 27 May 2022; Received in revised form 9 June 2022; Accepted 8 August 2022
Available online 10 August 2022

functions of fresh products and thus affect the beneficial effects (Li et al., 2010). Nowadays, in fulfilling the demands and preferences of consumers for choosing foods and medicines that promote health, knowledge regarding the biologically active compounds in products is significant. Thus, for a proper quality assessment of FSG during processing, comprehensive analysis of chemical substances is required.

Phosphodiesterase 4 (PDE4) is cAMP specific and abundantly expressed in inflammatory and immune cells, has been recognized as a key effector in inflammation responses (Francis et al., 2011). Inhibition of PDE4 leads to accumulation of intracellular cAMP and shift the balance of anti-inflammatory/pro-inflammatory. Therefore, PDE4 has been developed as a key regulator and important target for treating inflammatory disorders, such as psoriasis (X. Zhang et al., 2019), atopic dermatitis (Purushothaman et al., 2018) and rheumatoid arthritis (Y. He et al., 2020), *etc*. Flavonoids are well-known for their antioxidant and anti-inflammatory activities (Wu et al., 2020), and reported to exhibit directly or indirectly inhibitory activity on PDE4 (Ko et al., 2004). In view of this, investigating the anti-inflammatory effect of FSG based on PDE4 inhibition activity is of great significance for better understand the beneficial physiological effects and underlying mechanism.

Here, we hypothesize that traditional heat processing could affect the chemical profile and bioactivity of FSG, and the objective of the present study is therefore to evaluate its anti-inflammatory effect and explore the underlying mechanism. Ultra-high-performance liquid chromatography (UHPLC) coupled with quadrupole time-of flight mass spectrometry (QTOF-MS/MS) was utilized to characterize the chemical profiles of FSG and PSG. Data mining was performed using the principal components analysis (PCA) and orthogonal partial least square method-discriminant analysis (OPLS-DA) to explore the biomarkers of FSG and PSG. Meanwhile, quantification study was carried out to investigate the isomerization of chemical markers. Subsequently, the potential active compounds were confirmed by affinity ultrafiltration coupled with high resolution mass spectrometry, *in vitro* enzymatic assay and *in silico* study. At the same time, the anti-inflammatory effects of FSG and PSG were evaluated through the PDE4 enzyme inhibition assay. Overall, it is the first time that experimental and computational methods have been used to evaluate FSG during processing, which forms a basis for better food selection, improves nutritional recommendations that may prevent inflammation, thereby providing scientific rationale for the health benefits of this plant in related problems.

Materials and methods

Material

Eight batches of fresh medicinal herbs SG were collected from different herbal markets or harvested from various habitats in Macau, Guangdong and Guangxi provinces of China. The collected samples were identified by Prof. Hao Zhang of West China School of Pharmacy, Sichuan University, China. All authenticated samples were stored in the laboratory of Macao University of Science and Technology. Astilbin, neoastilbin, neoisoastilbin and isoastilbin at over purity greater than 98 % were purchased from Chengdu Push Bio-Technology Co. ltd. (Chengdu, China). Human PDE4 (Cat#60401, BPS Bioscience Inc, USA) and Nanosep Centrifugal Devices 10 K centrifugal filter devices provided by Millipore Co. ltd (Bedford, MA, USA) were used for bio-affinity study. The PDE4 inhibition assay kit (Cat#79558, BPS Bioscience Inc, USA) was used for PDE4 inhibition study. LC–MS grade acetonitrile, methanol and formic acid were bought from Fisher Scientific (Geel, Belgium). Ultrapure water was generated using the Milli–Q Advantage A10 System from Millipore GmbH (Schwalbach, Germany). All the other reagents used in the experiment were analytical grade, unless otherwise specified.

Sample preparation

The fresh rhizomes of different batches of SG were separately cut into 0.3–0.5 cm-thick slices, respectively, these slices were mixed freely and divided into two parts. Firstly, 100 g of fresh materials were suspended in 100 mL water, squeezed as juice by a juicing machine, and further freeze-dried to get FSG. Then, another section of fresh material (100 g) was dried in an oven (Nüve FN055 Ankara, Turkey, 55 L volume) at 55 ℃. The final weight of the slices varied in the range of 3–5 % after being weighed twice. Then the dried SG was reflux-extracted twice with water for 1 h each, the filtrate was combined and evaporated under vacuum, then freeze-dried to get PSG.

FSG and PSG were accurately weighed (10 mg), respectively, re-suspended with 10 mL 80 % methanol and extracted using ultrasonic/microwave-assisted extraction for 30 min. Supernatant was collected by centrifugation (8000 rpm for 10 min), filtered through a 0.22 μm PTFE syringe filter and stored at 4℃ prior to the UHPLC-MS/MS analysis. Stock solutions for each standard, including astilbin, neoastilbin, neoisoastilbin and isoastilbin were prepared by dissolving appropriate amounts of them in methanol to form 1 mg/mL, and immediately stored in darkness at −20 °C. Working solutions were prepared from the stock solutions using methanol by serial dilution.

Instrumentation and UHPLC-MS/MS conditions

Chromatographic analysis was performed on an Agilent 1290 UHPLC system (Agilent Technologies, Waldbronn, Germany). Separation was performed on a 2.1 × 100 mm, 1.8 μm ACQUITY HSS T_3 column (Waters, USA). The mobile phase was consisted of 0.1 % formic acid - water (A) and acetonitrile (B) with the following gradient: 0–5 min, 36 % B; 5–8 min, 36–95 % B. The flow rate was set at 0.3 mL/min, injection volume was 1 μL, and the column temperature was maintained at 35 °C.

The targeted MS/MS data were collected in negative ESI mode by Agilent 6550 QTOF-MS/MS (Agilent Technologies, Santa Clara, CA, USA) to achieve better peak separation. The MS parameters were set as follows: gas temperature = 300 °C, nebuliser pressure = 30 psi, drying gas flow velocity = 12 L/min, sheath gas temperature = 350 °C, capillary voltage = 3000 V, and nozzle voltage = 2500 V. The collision energy was fixed to 35 eV for automated and target MS/MS analysis.

Quantification of astilbin, neoastilbin, neoisoastilbin and isoastilbin were carried out on an Agilent 6460 Triple Quadrupole (QQQ) MS/MS (Agilent Technologies, Santa Clara, CA, USA). The mass parameters were set as follows: drying gas temperature and gas flow rate were 350 °C and 11 L/min, nebulizer pressure of 45 psi, sheath gas temperature at 250 °C and flow was set at 11 L/min, capillary voltage of 3500 V and nozzle voltage was 500 V. Analyte detection was carried out by multiple reaction monitoring (MRM) mode using a positive ESI interface. The optimized MRM fragmentation transitions were m/z 449.2 → 303.0 and m/z 449.2 → 285.0 for both astilbin and its isomers. Fragmentor voltage was set at 160 V, collision energy at 15 V, and the dwell time was set at 100 ms for each transition.

Data mining and multivariate statistical analysis

The multivariate statistical analysis was carried out to visualize the characteristic components in FSG and PSG by using SIMCA–P software (version 14.0 Umetrics, Umea, Sweden). Firstly, the obtained raw data were organized and processed using Mass Hunter Workstation software (Agilent Technologies, version B.06.00). A series of procedures in the software were used to handle a chromatogram from 1 to 15 min, the retention time of 0.1 min, the mass range of 100–1000 Da, MS tolerance was 0.1 Da, and the noise elimination level of 10.00 %. Then, the extracted data exported as CEF formatted file, which can be analyzed by the statistic Mass Profiler Professional software package 2.0 (Agilent Technologies). The next step involves aligning the features using an internal standard. Finally, for baseline correction, all compounds were

treated with the calculated representative value (Ma et al., 2020). The final data with accurate quality and retention time determined in FSG and PSG were imported into SIMCA-P to select specific biomarkers using PCA and OPLS-DA. Potential biomarkers were selected according to Variable importance in the Project (VIP) value and the S–plot.

Screening of potential PDE4 inhibitors from FSG

The screening procedures were carried out with ultrafiltration device, following the previous report with slight adjustments (Jiao et al., 2019). For ultrafiltration, FSG (1.0 mg/mL, 5 μL) was mixed with 295 μL phosphate buffer (pH 7.0) containing 10 ng/μL, 50 ng/μL and 100 ng/μL human recombinant PDE4 enzyme, respectively. Inactivated PDE4 (heated with boiling water for 10 min) was prepared in parallel as blank control group. All the samples were incubated at 37 °C for 30 min. After incubation, the mixtures were then transferred to a centrifugal ultrafiltration column with 10 kDa cut-off membrane and centrifuged at 8,000 × g for 10 min at 4℃. The samples were washed twice with 100 μL phosphate buffer to remove unbound components. Subsequently, transfer the filter to a new centrifuge tube to make the ligands cleaved from PDE4 using 100 μL methanol/water (80:20; *v/v*). The dissociated ligands were gathered after centrifugation for three times (10,000 × g, 10 min), then dried under a nitrogen gas, and reconstituted in 100 μL 60 % methanol (*v/v*) for PDE4 inhibitory ability evaluation and active compounds identification by UHPLC–QTOF–MS/MS analysis.

The bio-affinity degree measured by UHPLC–QQQ–MS/MS therefore represents the specific binding of inhibitors to PDE4 (S. Li et al., 2021). It was calculated as follows: Bio-affinity degree (%) = $(A_1\text{-}A_2/A_0) \times 100$ %, where A_1, A_2 and A_0 represent the amounts of screened compounds in FSG with activated PDE4, inactivated PDE4 and without PDE4, respectively.

In vitro PDE4-inhibitory assay

The commercially available assay kit was used for PDE4 inhibition study with fluorescein-labelled cAMP (FAM-cAMP) as substrate, and materials including PDE assay buffer, binding agent diluent (cAMP) and binding agent. 1,4-Dithiothreitol (DTT) was obtained from Aladdin Industrial Corporation (Shanghai, China). Apremilast used as the positive control was purchased from Sigma Aldrich. Briefly, the test compound was dissolved in assay buffer with low concentration of DMSO (10 %, *v/v*), then, 5 μL of the dilution sample was added to a 50 μL reaction. Subsequently, the enzymatic reactions which composed of blank, substrate control, sample analysis and positive control were incubated for an hour containing PDE4 enzyme, 200 nM FAM-cAMP and PDE assay buffer at room temperature. Next step, 100 μL of binding agent/binding agent diluent (1:99; *v/v*) was added to each reaction, and incubating for 30 min at room temperature with slow shaking before fluorescence polarization measurement by Spectramax iD5 multi-mode microplate reader (Molecular Devices, USA). The wavelength of fluorescence polarization was set within 5 nm bandwidth for excitation at 485 nm and within 10 nm bandwidth for 528 nm emission. The PDE4 activity experiment was conducted in triplicate at each concentration.

The initial concentrations of FSG and PSG were screened. The concentration that provided more than 95 % PDE4 inhibitory activity was further studied, which could inhibit 50 % of enzyme activity (IC_{50}). Therefore, the final levels of the SG extracts that between 1000 mg/mL to 1 mg/mL were applied. Meanwhile, the PDE4 inhibitory activity of astilbin and its isomers (neoasitilbin, neoisoastilbin and isoastilbin) were conducted, ranging from 2.5 mg/mL to 0.001 mg/mL. The fluorescence polarization data were analyzed, and IC_{50} values were calculated by fitting the data points with the dose–response function using GraphPad Prism version 7.0 (San Diego, CA, USA). Finally, the percentage (%) activity of each sample was calculated using the following equation: % activity = (FP − FPb)/(FPt − FPb) × 100 %, where FP, FPt, FPb were the fluorescence polarization in the presence of the compound, the fluorescence polarization in absence of the compound and fluorescent polarization in the absence of both PDE and the compound, respectively.

In silico analysis

Docking calculation was performed using Autodock Vina software (version 1.12) by the Lamarckian genetic algorithm (Morris et al., 1998). The 3D structure of astilbin, neoastilbin, isoastilbin and neoisoastilbin were optimized for energy minimization by ChemOffice 19.0. The crystal of PDE4 found in the RCSB Protein Data Bank (PDB ID: 1xmy) (Y. Li et al., 2018) were used for the alignment between astilbin and its isomers, respectively. The ligands and waters were removed from the protein using Pymol software. Polar hydrogen atoms were added, and Geisteger charges were assigned to the receptor protein by means of Auto Dock Tools version 1.5.6. A grid box was prepared for PDE4 to cover the binding site with size of 118 × 126 × 126 Å, the spacing of 1 Å, centered at coordinate ×, y, z 42.73, 2.65, 51.68. The saved file in the PDBQT format was used as an input in Auto Dock Vina. To increase the docking accuracy, the value of exhaustiveness was set to 120, and the number of final conformations generated was set to 20. Ligand (R)-Rolipram was extracted from PDE4 to validate the docking scoring procedure and then docked back into PDE4 *via* the same conditions described above. The Pymol software was used to calculate the root-mean-square deviation (RMSD) between the optimal redocking of the ligand and the original conformation.

Results and discussion

Metabolites profiles analysis of FSG and PSG

UHPLC-QTOF-MS/MS is a powerful tool for characterization of complex chemical mixtures from plant origin matrix. In present study, a comprehensive profile of metabolites of FSG and PSG were described using the metabolomic approach. A total of twenty-four compounds (Table 1) were either identified or tentatively characterized based on matching the molecular formulas, quasi-molecular ions, and fragment ions, as well as retention times with those of reference compounds and published data (L. He et al., 2018)(X. He et al., 2016). Among which, neoastilbin, astilbin, neoisoastilbin and isoastilbin were proved to be the major components in SG, eluted at 3.60, 3.76, 4.33 and 4.50 min in the base peak ion (BPI) chromatograms, respectively (Fig. 1A). Their structures were unambiguously confirmed by comparing the retention time and fragmentation mode with those of standard compounds. For instance, on the MS spectra of astilbin, ions at *m/z* 449.1090 Da was corresponding to the deprotonated molecular ion $C_{21}H_{21}O_{11}$ $[M-H]^-$. Fragment ions information at *m/z* 303.0504, 285.0402 and 151.0033 produced with collision induced dissociation under high energy (45 eV) ascribed to a typical flavonoid aglycone. The fragment ion at *m/z* 303.0504 was generated by loss of a rhamnose residue and further fragmented to yield product ions at *m/z* 285.0402 and 125.0237 by loss of H_2O and $C_6H_6O_2$. The ion at *m/z* 151.0033 was generated after Retro–Diels Alder cleavage (loss of a $C_8H_8O_3$) (Gu et al., 2015). Neoastilbin, neoisoastilbin and isoastilbin were isomers that showed different retention times but had fragmentation pattern identical to that of astilbin.

As shown in the BPI chromatograms (Fig. 1A), a total of nine peaks were found in both FSG and PSG. Interestingly, components such as 4-hydroxy-5-(3′,4′,5′-trihydroxyphenyl)-valeric acid-O-methyl-O-glucuronide, epicatechin, tufulingoside, naringenin-7-O-β-D-glucoside, isohemiphloin, iristectorin A, tricin 5-O-β-D-glucoside, tricin 5-O-β-D-glucoside, eupatolin, smiglaside E and smiglaside B (peak 3, 5, 7, 13, 14, 15, 17, 18, 19, 23 and 24, respectively), could not be monitored in FSG due to their lower contents, which may be related to thermal treatment that disrupt the cell wall and liberate more flavonoid in PSG (Choi et al., 2006). Nevertheless, glucosyringic acid, smiglanin and iristectorin B

Table 1
The compounds identified in the BPI chromatogram of *Smilax glabra* (SG) extracts.

Peak No.	Retention (min)	$[M-H]^-$ (error, ppm)	MS/MS Fragments Ions	Molecular Formula	Identification
1	1.15	461.1305 (2.2)	241.0021, 167.0346, 152.0111, 123.0444, 108.0209	$C_{19}H_{26}O_{13}$	Sibiricose A
2	1.27	359.0976 (2.5)	197.0456, 182.0220, 166.9984,153.0555, 138.0320, 123.0084	$C_{15}H_{20}O_{10}$	Glucosyringic acid
3	1.30	447.1134 (-1.1)	271.0975, 256.0735, 225.0777, 197.0456, 182.0218, 166.9985	$C_{18}H_{24}O_{13}$	4-Hydroxy-5-(3′,4′,5′-trihydroxyphenyl)-valeric acid-O-methyl-O-glucuronide
4	1.99	289.0707 (-1.7)	245.0807, 203.0696, 151.0388, 125.0232	$C_{15}H_{14}O_6$	Catechin
5	2.44	289.0716 (0.8)	245.0810, 203.0705, 151.0389, 125.0228	$C_{15}H_{14}O_6$	Epicatechin
6	2.88	339.0715 (-0.3)	248.9486, 193.0132, 136.0159	$C_{15}H_{16}O_9$	Smiglanin
7	2.91	339.0716 (0)	285.0397, 193.0135, 151.0030, 136.0159, 125.0234, 108.0206	$C_{15}H_{16}O_9$	Tufulingoside
8	3.60	449.1090 (1.3)	303.0503, 285.0400, 151.0033, 125.0236	$C_{21}H_{22}O_{11}$	Neoastilbin*
9	3.76	449.1090 (1.3)	303.0504, 285.0402, 151.0033, 125.0237	$C_{21}H_{22}O_{11}$	Astilbin*
10	4.33	449.1084 (0)	303.0500, 285.0396, 151.0031, 125.0235	$C_{21}H_{22}O_{11}$	Neoisoastilbin*
11	4.50	449.1088 (0.9)	303.0497, 285.0394, 151.0031, 125.0235	$C_{21}H_{22}O_{11}$	Isoastilbin*
12	4.81	433.1132 (-0.7)	269.0443, 259.0601, 180.0054, 152.0107, 151.0031, 125.0231	$C_{21}H_{22}O_{10}$	Engeletin
13	4.89	433.1133 (-0.5)	269.0446, 259.0596, 180.0057, 152.0108, 125.0235	$C_{21}H_{22}O_{10}$	naringenin-7-O-β-D-glucoside
14	5.47	433.1127 (-1.8)	269.0437, 259.0607, 180.0053, 152.0104, 125.0231	$C_{21}H_{22}O_{10}$	Isohemiphloin
15	5.49	491.1187 (-0.6)	285.0394, 175.0394, 151.0029, 125.0232	$C_{23}H_{24}O_{12}$	Iristectorin A
16	5.56	491.1197 (1.4)	328.9729, 285.0394, 180.0058, 151.0029, 125.0236	$C_{23}H_{24}O_{12}$	Iristectorin B
17	5.58	491.1188 (-0.4)	285.0391, 180.0053, 151.0029	$C_{23}H_{24}O_{12}$	tricin 5-O-β-D-glucoside
18	5.64	491.1195 (1.0)	285.0395, 180.0053, 151.0031	$C_{23}H_{24}O_{12}$	tricin 7-O-β-D-glucoside
19	5.71	491.1194 (0.8)	285.0398, 180.0054, 151.0032	$C_{23}H_{24}O_{12}$	eupatolin
20	5.80	491.1190 (0)	285.0390, 180.0051, 151.0031	$C_{23}H_{24}O_{12}$	unknown
21	5.87	491.1198 (1.6)	285.0397, 180.0055, 151.0030	$C_{23}H_{24}O_{12}$	unknown
22	6.13	401.0867 (-1.5)	211.1322, 183.0112, 152.0111, 123.0448	$C_{20}H_{18}O_9$	Frangulin B
23	6.24	923.2641 (3.4)	882.2593, 863.2395, 777.2310, 421.2264, 325.1836, 311.1684	$C_{45}H_{48}O_{21}$	Smiglaside E
24	6.35	965.2723 (0.8)	923.2596, 905.2493, 819.2338, 789.2258, 747.2133, 729.2038, 483.1302, 175.0404, 145.0287	$C_{46}H_{50}O_{22}$	Smiglaside B

Error (ppm): the difference between experimental mass and theoretical mass of the compound; * indicated compounds 8, 9, 10 and 11 were confirmed by chemical reference standards.

(peaks 2, 6 and 16) could only be detected in FSG, and the peak intensities of smiglanin, astilbin, iristectorin B and frangulin B (peak 6, 9, 16 and 22) in FSG were significantly stronger than that in PSG. This observation could probably be ascribed to the various content of compounds in FSG and PSG, to evaluate the constituent differences between the two groups, other chemometric analysis were subsequently carried out.

Chemometrics based analysis for identifying the biomarkers of FSG and PSG

Multivariate data analysis was used to better visualize the subtle similarities and differences between FSG and PSG. PCA is applied as an unsupervised clustering method to identify patterns in data to reduce dimensionality. It can describe independent changes in results by defining a limited number of principal components(Su et al., 2019). After Pareto scaling with mean centering, the PCA data were displayed as scores plot (Fig. 1B). The first two principal components PC1 and PC2 accounted for 44.5 % and 27.1 % of the total variance, and the model fitness parameters were 0.697 for R2X (cum) and 0.334 for Q2 (cum), suggesting that the established PCA model had good fitness and prediction (Worley & Powers, 2016). The score plot showed that the identified samples were clearly clustered into two groups, indicating that the processing procedures resulted in changes in the composition and/or content of the compounds. In addition, the overlap of FSG samples may be related to the highly similar compounds before processing.

To recognize potential chemical markers that distinguish FSG from PSG, we performed an extended statistical analysis of the OPLS-DA model. Typically, each point represents an exact mass retention time (t_R–*m/z*). The X-axis represents the variable contribution, while the Y-axis indicates the sample correlation. Thus, the further away from the zero value, the stronger this point was affected to the group difference. So, the t_R–*m/z* pairs on both ends of the "S" represent the most confident markers for each group. In addition, the contribution of candidate marker compounds to variation and correlation in the dataset was also checked by using the VIP score of OPLS-DA. The four t_R–*m/z* marked in red with the high VIP were identified as candidate markers by using VIP and S-plot (Fig. 1C). For instance, compound **8** (neoastilbin, tR 3.60 min, *m/z* 449.1090, VIP 3.31), and compound **10** (neoisoastilbin, t_R 4.33 min, *m/z* 449.1084, VIP 3.90), in the bottom left corner of S represent the ions that contribute the most to the difference between FSG and PSG. Similarly, the other compounds, compound **9** (atilbin, t_R 3.76 min, *m/z* 449.1090, VIP 3.17), and compound **11** (isoastilbin, t_R 4.50 min, *m/z* 449.1088, VIP 1.41) at the top right corner of S also contribute significantly to the difference. Therefore, four astilbin isomers could be used as potential chemical markers to differentiate between FSG from PSG.

Quantification of chemical markers in FSG and PSG

To further characterize the chemical markers, we employed a sensitive quantitative UHPLC–QQQ–MS/MS method. The average content of astilbin in eight batches of FSG was 0.52 % (Table 2), while in PSG was 0.15 %, which was about three times lower than that of FSG. It's noteworthy that none of the PSG samples met the limit requirements of Chinese Pharmacopoeia (should be greater than 0.45 %), this might be resulted from its decomposition and/or isomerization after heating (Zheng et al., 2018). Similarly, the content of isoastilbin was shown reducing to 0.04 % in PSG compared with that of FSG (0.13 %). Regarding neoisoastilbin and neoastilbin, the average contents in PSG

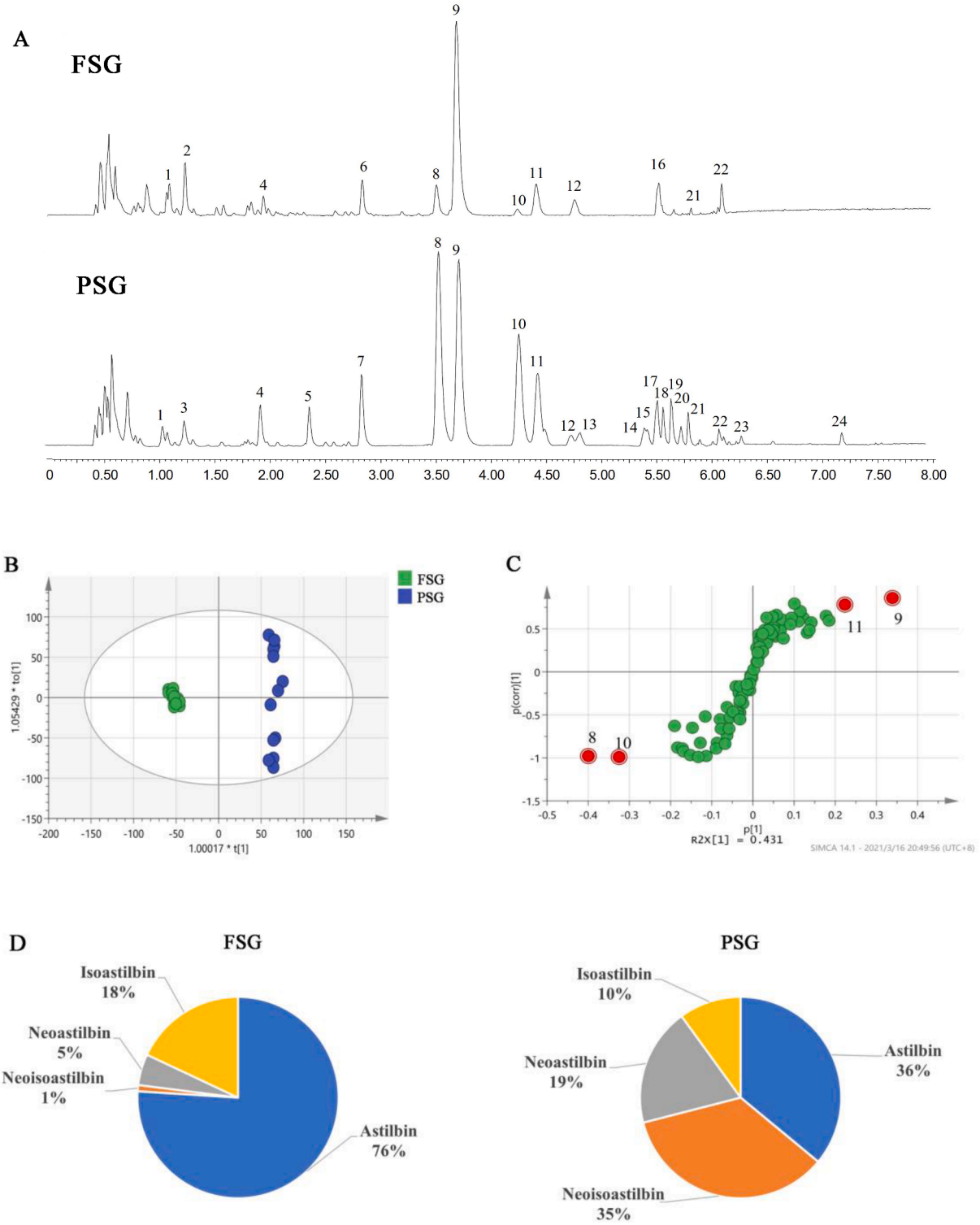

Fig. 1. (A) UHPLC-QTOF-MS base peak intensity chromatograms of fresh and processed *Smilax glabra* (FSG and PSG) in negative ion mode. (B) PCA score plot and (C) S–plot of FSG and PSG. Compounds: 8, neoastilbin; 9, astilbin; 10, neoisoastilbin; 11, isoastilbin. (D): Pie charts of the proportion of astilbin isomers in FSG and PSG. Calculations were based on UHPLC–QQQ–MS/MS data.

were 0.15 % and 0.08 %, respectively, which were significantly higher than that of FSG (0.05 % and 0.03 %, respectively). The pie chart of the content ratios of astilbin and its isomers in each group (Fig. 1D) showed the content changes more intuitively. Apparently, after exposed to heating for a period, the contents of astilbin and isoastilbin were decreased significantly in PSG, and on the contrary, the levels of neoastilbin and neoisoastilbin were increased. Since the contents of flavonoids may be related to the bioactive potency (Kasai et al., 1991), another consideration is that different isomer contents may lead to changes in the bioactivity of FSG after heat processing.

Screening of potential PDE4 inhibitors from FSG

The affinity ultrafiltration combined with mass spectrometry

Table 2
Contents (%) of astilbin and its isomers in SG based on heated processing (n = 8).

Sample	Neoastilbin	Astilbin	Neoisoastilbin	Isoastilbin
FSG	0.03 ± 0.03	0.52 ± 0.11	0.05 ± 0.001	0.13 ± 0.03
PSG	0.08 ± 0.04*	0.15 ± 0.05**	0.15 ± 0.04**	0.04 ± 0.05*

Values are expressed as means ± S.D. *$P < 0.05$, **$P < 0.01$ (Student's two-independent-sample *t*-test), significantly different from those by FSG.

technology has been reported to be a reliable tool for screening of protein-binding compounds with binding affinities from complex matrix (Wang et al., 2020). In this study, FSG was incubated with PDE4, the potential PDE4 inhibitor could be identified after separating the unbound small molecules from PDE4 binding complex by the ultrafiltration membrane. Potential enzyme inhibitors were assessed by incubating a fixed concentration of FSG (1 g/mL) with different concentrations (10, 50 and 100 μg/mL) of PDE4. Only compounds with certain binding ability to PDE4 could be detected after ultrafiltration. The screening results (Fig. 2) showed that four compounds identified as neoastilbin (peak **8**), astilbin (peak **9**), neoisoastilbin (peak **10**) and isoastilbin (peak **11**) were found to be PDE4 binders by comparison of the chromatogram with the negative control (FSG extract). The bio-affinity degree was introduced to further understand the relative enzyme binding capacity (S. Li et al., 2021). Generally, a higher value means that the compound has a higher binding ability or a higher enzyme inhibitory activity. From the contributing inhibitors of PDE4 in FSG (Table 3), astilbin was the dominant compound with the highest binding ability.

PDE4 enzyme inhibition activity

PDE4 enzyme inhibition assay was conducted to investigate the biological activities of four astilbin isomers, FSG and PSG, respectively. Generally, the larger the IC_{50} value, the weaker enzyme inhibition ability (Brooks et al., 2012). In this study, PDE4 inhibitor Apremilast was used as positive control with an IC_{50} value of 43.35 nM (Table 3), which was similar to previous report (Kitzen et al., 2018). Four astilbin isomers showed varying degrees of PDE4 inhibition capacity, among

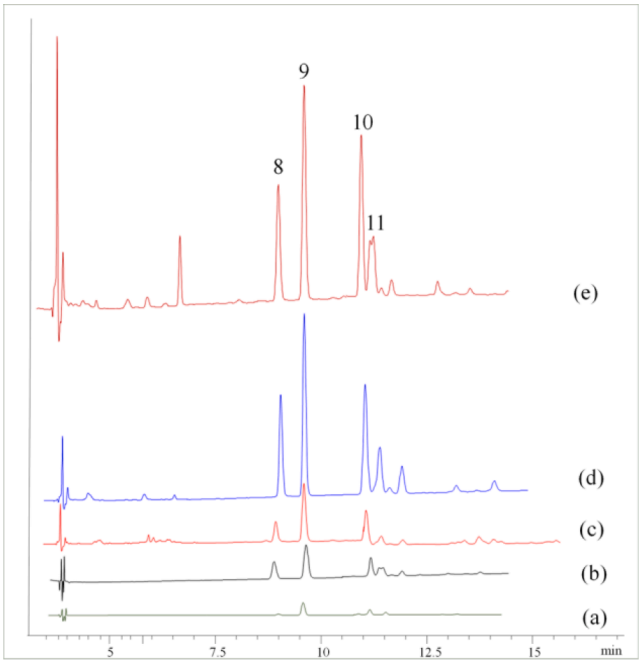

Fig. 2. Compounds determined to be ligands of PDE4 using affinity ultrafiltration UHPLC–QTOF–MS/MS. PDE4 concentration: (a) With inactivated PDE4; (b) 10 ng/μL; (c) 50 ng/μL; (d) 100 ng/μL; (e) FSG extract. Peaks: 8, neoastilbin; 9, astilbin; 10, neoisoastilbin; 11, isoastilbin.

Table 3
Bio-affinity degree (%) and IC_{50} values with PDE4.

Analytes	10 ng/μL	50 ng/μL	100 ng/μL	IC_{50}
Neoastilbin	11.22 ± 0.27	17.89 ± 0.26	20.10 ± 0.21	43.03 ± 2.9 μM
Astilbin	22.13 ± 0.40	31.24 ± 0.19	42.29 ± 0.33	14.44 ± 0.7 μM
Neoisoastilbin	8.14 ± 0.52	12.87 ± 0.54	14.86 ± 0.42	103.28 ± 4.1 μM
Isoastilbin	5.41 ± 0.27	11.11 ± 0.13	15.13 ± 0.22	129.57 ± 3.8 μM
FSG				0.009 ± 0.01 μg/μL
PSG				0.110 ± 0.03 μg/μL
Apremilast				43.35 ± 4.5 nM

Each value represents the mean ± S.D. of 3 – 5 experiments.

which astilbin had the lowest IC_{50} value (14.44 μM), followed by neoastilbin (43.03 μM), neoisoastilbin (103.28 μM) and isoastilbin (129.57 μM). As expected, these isomers showed significant differences in IC_{50} values for PDE4 inhibitory. These results indicated that the affinity ultrafiltration mass spectrometry technology method could successfully screen out the potential PDE4 inhibitors from FSG. Additionally, the IC_{50} of FSG was 0.009 μg/μL, which was about 12 times higher than that of PSG (0.110 μg/μL).

The interaction of four astilbin isomers with PDE4 via molecular docking

Molecular docking was conducted to reveal the interaction between astilbin isomers and PDE4. The inhibitory ability of the isomers against PDE4 could be affected by the number of H-bonds and active residues of the protein–ligand complex (Xie et al., 2021). Astilbin showed the strongest interactions with PDE4 (Fig. 3), with four amino acid residues (Gln443, Asp392, Glu304 and His234) involved in the formation of five H-bonds (with average distance of 2.92 Å). Isoastilbin, showing four H-bonds (average distance of 3.28 Å) interactions with four amino acid residues (Ser429, Met347, Glu304 and His278) of PDE4. The number of three H-bonds and amino acid residues (Gln443, Thr345 and Glu304) were formed in neoastilbin-PDE4 complex (with H-bond distance ranging between 2.7 Å and 2.9 Å), the same H-bonds numbers were found in neoisoastilbin-PDE4 complex, with three residues (Met347, Glu304 and Tyr233) of the receptor (average distance of 3.13 Å).

It had been reported that the formation of hydrogen bonds increases the hydrophobicity of the ligand–protein complex but reduces the hydrophilicity, thereby increasing the binding affinity and stability of the complex (Roy et al., 2017). On comparison of the estimated binding affinity between PDE4 and the isomers, we found that astilbin had the most negative value with −9.6 kcal mol^{-1}, followed by neoastilbin −9.1 kcal mol^{-1}, neoisoastilbin −8.7 kcal mol^{-1} and finally isoastilbin −8.3 kcal mol^{-1}. This can be directly related to the number of hydrophobic/hydrogen bonds interactions that these isomers undergo with the surrounding PDE4 residues. Moreover, the H-bond interaction with Gln443 and π − π stacking on Phe446 (Fig. 3B) were observed in astilbin-PDE4 complex, while these interactions were not involved in the binding of other three isomers. In addition, for (R)-Rolipram re-docked into the binding pocket of PDE4 and the RMSD between a docked pose and the crystal pose was 1.375 Å (Supplemental Fig. S1), further indicates that the docking program is accurate.

Discussion

In this work, a combination of mass spectrometry technology and chemometrics statistical method provided to be an effective and practical tool favoring to analysis the chemical profiles and identify the potential biomarkers of FSG and PSG. Then, quantification of the chemical markers, astilbin, neoastilbin, neoisoastilbin and isoastilbin,

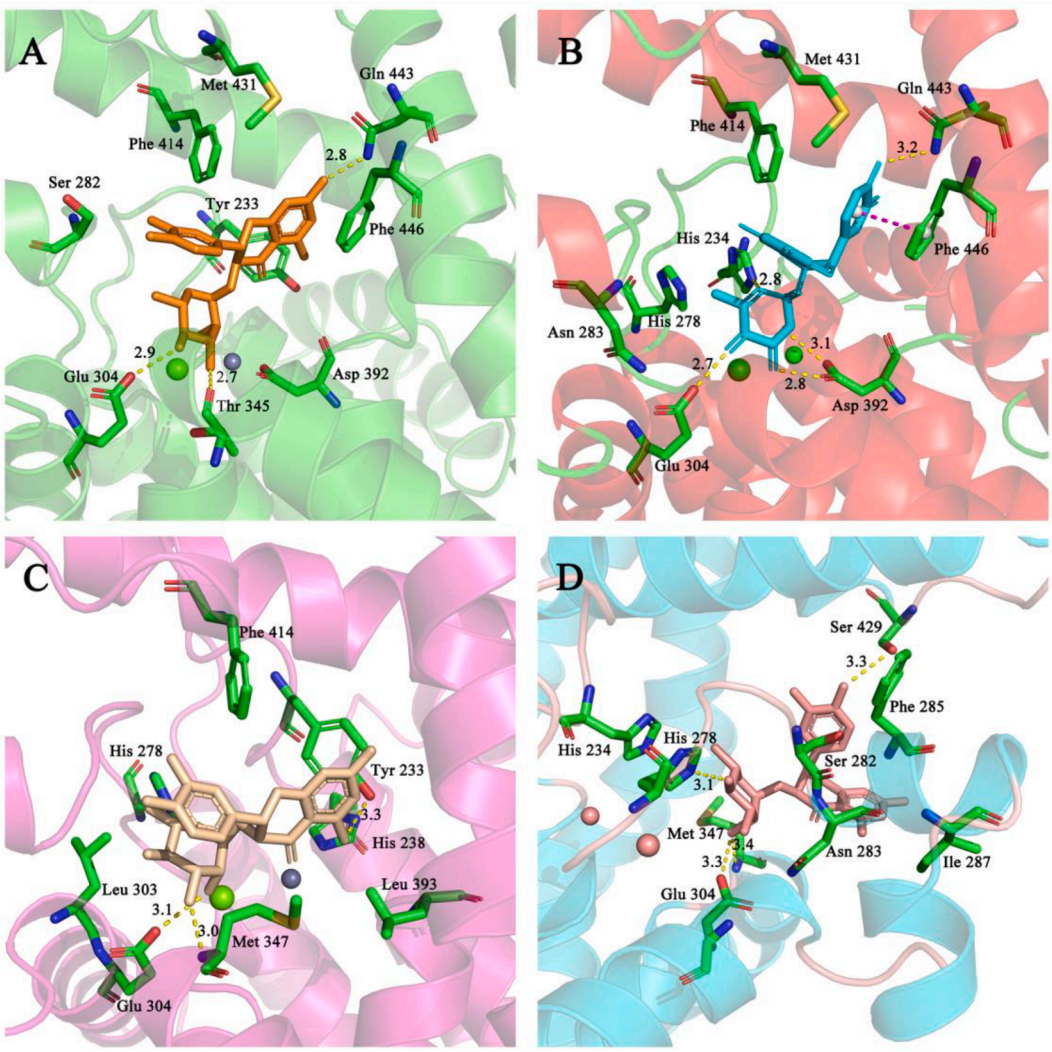

Fig. 3. The conformations of (A) neoastilbin, (B) astilbin, (C) neoisoastilbin and (D) isoastilbin docked with PDE4 with residues in the active sites. The yellow dotted lines indicating hydrogen bonds, and dashed magenta line denotes π-π stacking. (For interpretation of the references to colour in this figure legend, the reader is referred to the web version of this article.)

revealed that their contents changed significantly after herb heating process of SG. In-depth study found that heating promoted the interconversion between astilbin and its isomers, *e.g.*, astilbin and neoastilbin were isomerized into their cis–trans-isomer, namely neoisoastilbin and isoastilbin, respectively, *vice versa* (Supplemental Fig. S2), which was similar to that of previous study (Zheng et al., 2018). Actually, the stability of astilbin was temperature dependent, and isomerization of astilbin (2R, 3R) could relate to the ring opening and resulting in formation of quinone methide. After that, the quinone methide can be recyclized to form neoisoastilbin (2S, 3R), or through the epimerization of α-hydroxychalcone, and finally to form isoastilbin (2R, 3S) and neoastilbin (2S, 3S) *via* recyclization (Structure shown in Fig. S3) (Zheng et al., 2018) (Gaffield et al., 1975). Therefore, we can conclude that herb heat processing plays a key role in chemical profiles, which strongly affects the isomerization of astilbin, resulting in significant content changes in four astilbin isomers.

Four astilbin isomers were identified as potential PDE4 inhibitors from FSG by using the affinity ultrafiltration combined with mass spectrometry method, which has been demonstrated for high-throughput screening and identification of bioactive components in plant extracts (S. Li et al., 2022). According to bio-affinity theory, ligands are incubated with PDE4 (receptor) to form receptor-ligand complexes. After ultrafiltration, unbound molecules were removed and the released ligands from the binder were characterized using mass spectrometry. The results showed that four astilbin isomers have different binding abilities to PDE4, as the enzyme concentration increases, the peak intensity enhanced. Among them, astilbin was the dominant compound with the highest binding ability, therefore, the four astilbin isomers of FSG, especially astilbin, determined PDE4 inhibitory activity to a large extent.

The four astilbin isomers showed different inhibitory activities on PDE4 according to the *in vitro* PDE4 inhibition assay, among which astilbin had the highest inhibitory effect (IC_{50} = 14.44 μM), gave 2.9-, 7.1- and 8.9-fold higher than that of neoastilbin (IC_{50} = 43.03 μM), neoisoastilbin (103.28 μM) and isoastilbin (129.57 μM), respectively, the results were consistent with affinity ultrafiltration mass spectrometry. This highly suggests that the distinct PDE4 inhibitory activities between astilbin and its isomers might be ascribed to the different structural configurations, which affect the interaction of functional groups with PDE4 enzyme (Z. Li et al., 2013).

Molecular docking was further conducted to reveal the potential protein–ligand interaction of four isomers with PDE4. Based on the structure–activity relationship analysis, the C'-3 hydroxyl group of B-ring of flavonoid was very important for PDE4 inhibition (Ko et al., 2004). The superposition structures (Supplemental Fig. S4) of four astilbin isomers within the active site pocket of PDE4 indicated that the

B-rings of neoastilbin, neoisoastilbin and isoastilbin showed a significant shift from astilbin. However, in astilbin-PDE4 complex, the functional group at C'-3 position of astilbin interacts hydrogen bond with Gln443, and π-π stacking on Phe446 with aromatic B-ring, which were characteristic binding modes of many PDE4 inhibitors (Z. Li et al., 2013). Therefore, we found that astilbin interacts with PDE4 differently from other isomers and has a stronger binding affinity, which agreed with the *in vitro* enzymatic assay results and affinity ultrafiltration mass spectrometry.

The above results demonstrate that this combinatorial approach including affinity ultrafiltration mass spectrometry, *in vitro* enzymatic assay and *in silico* analysis was successfully established for the rapid and efficient discovery of potential PDE4 inhibitors from FSG. Therefore, we can conjecture that the inhibition of PDE4 by the major ingredient astilbin, accounts for most of the inhibiting PDE4 activity of FSG, although other compounds such as neoastilbin, neoisoastilbin and isoastilbin also contribute.

According to the PDE4 enzyme inhibition activity, FSG (IC_{50} = 0.009 μg/μL) exhibit about 12-fold stronger inhibitory activity than PSG (IC_{50} = 0.110 μg/μL) on PDE4 inhibition, indicating a significant decrease in biological activity after heat processing. Regarding the major contributor of PDE4 inhibition, astilbin, its content reduced from 0.52 % to 0.15 % during SG processing, and its inhibitory activity against PDE4 was about 7-fold higher than its cis–trans-isomer, neoisoastilbin, thus this direct evidence supports that change in biological activities of four astilbin isomers under processing might be responsible for the decreased PDE4 inhibitory activities of FSG. Taken together, during SG processing, heat-activated astilbin isomerization leads to different PDE4 inhibitory activities, resulting in the different anti-inflammatory activities of FSG and PSG.

Conclusion

For the first time, these results demonstrated that FSG exhibit a more potent anti-inflammatory effect on PDE4 inhibitory activity than PSG. Our work established an efficient and validated approach to support astilbin as the main active compound of FSG responsible for PDE4 inhibitory activity. We elucidated that herb processing strongly affected astilbin isomerization, which leads to significant changes in the contents and PDE4 inhibitory activities of four astilbin isomers, resulting in the decreased anti-inflammatory effect of FSG. This information helps explain the traditional usage of FSG for anti-inflammation and is valuable to form a foundation for better food selection, ultimately helping improve the appreciation of certain foods in the market.

CRediT authorship contribution statement

Youjiao Wu: Methodology, Software, Writing – original draft. **Lili He:** Formal analysis, Methodology, Writing – review & editing. **Yi Yang:** Methodology, Data curation. **Zhigang Yan:** Visualization. **Zhifeng Zhang:** Conceptualization, Investigation, Writing – review & editing. **Xiaojun Yao:** Software, Validation. **Pei Luo:** Conceptualization, Supervision, Writing – review & editing.

Declaration of Competing Interest

The authors declare that they have no known competing financial interests or personal relationships that could have appeared to influence the work reported in this paper.

Acknowledgments

This work was supported by the Grants from the Macau Science and Technology Development Fund (FDCT) (grant number 0122/2020/A to Zhifeng Zhang), Natural Science Foundation of Guangxi (No. 2018GXNSFAA281139 to Lili He), National Natural Science Foundation of China (No. 81960705 to Zhigang Yan).

Appendix A. Supplementary data

Supplementary data to this article can be found online at https://doi.org/10.1016/j.fochx.2022.100425.

References

Brooks, H. B., Geeganage, S., Kahl, S. D., Montrose, C., Sittampalam, S., Smith, M. C., & Weidner, J. R. (2012). Basics of enzymatic assays for HTS. *Assay Guidance Manual [Internet]*.

Choi, Y., Lee, S. M., Chun, J., Lee, H. B., & Lee, J. (2006). Influence of heat treatment on the antioxidant activities and polyphenolic compounds of Shiitake (Lentinus edodes) mushroom. *Food Chemistry, 99*(2), 381–387.

Francis, S. H., Blount, M. A., & Corbin, J. D. (2011). Mammalian cyclic nucleotide phosphodiesterases: Molecular mechanisms and physiological functions. *Physiological Reviews, 91*(2), 651–690.

Gaffield, W., Waiss, A. C., Jr, & Tominaga, T. (1975). Structural relations and interconversions of isomeric astilbins. *The Journal of Organic Chemistry, 40*(8), 1057–1061.

Gu, W., Li, N., Leung, E. L., Zhou, H., Yao, X., Liu, L., & Wu, J. (2015). Rapid identification of new minor chemical constituents from Smilacis Glabrae Rhizoma by combined use of UHPLC-Q-TOF-MS, preparative HPLC and UHPLC-SPE-NMR-MS techniques. *Phytochemical Analysis, 26*(6), 428–435.

He, L., Zhang, Z., Liu, Y., Chen, D., Yuan, M., Dong, G., … Yan, Z. (2018). Rapid discrimination of raw and sulfur-fumigated Smilax glabra based on chemical profiles by UHPLC-QTOF-MS/MS coupled with multivariate statistical analysis. *Food Research International, 108*, 226–236.

He, X., Yi, T., Tang, Y., Xu, J., Zhang, J., Zhang, Y., … Chen, H. (2016). Assessing the quality of Smilacis Glabrae Rhizoma (Tufuling) by colormetrics and UPLC-Q-TOF-MS. *Chinese Medicine, 11*(1), 1–9.

He, Y., Huang, Y., Mai, C., Pan, H., Luo, H.-B., Liu, L., & Xie, Y. (2020). The immunomodulatory role of PDEs inhibitors in immune cells: Therapeutic implication in rheumatoid arthritis. *Pharmacological Research*, 105134.

Hua, S., Zhang, Y., Liu, J., Dong, L., Huang, J., Lin, D., & Fu, X. (2018). Ethnomedicine, phytochemistry and pharmacology of Smilax glabra: An important traditional Chinese medicine. *The American Journal of Chinese Medicine, 46*(02), 261–297.

Jiang, J., & Xu, Q. (2003). Immunomodulatory activity of the aqueous extract from rhizome of Smilax glabra in the later phase of adjuvant-induced arthritis in rats. *Journal of Ethnopharmacology, 85*(1), 53–59.

Jiao, J., Yang, Y., Wu, Z., Li, B., Zheng, Q., Wei, S., … Yang, M. (2019). Screening cyclooxygenase-2 inhibitors from Andrographis paniculata to treat inflammation based on bio-affinity ultrafiltration coupled with UPLC-Q-TOF-MS. *Fitoterapia, 137*, Article 104259.

Kasai, R., Hirono, S., Chou, W., Tanaka, O., & Chen, F.-H. (1991). An additional sweet dihydroflavonol glycoside from leaves of Engelhardtia chrysolepis, a Chinese folk medicine, Huang-qi. *Chemical and Pharmaceutical Bulletin, 39*(7), 1871–1872.

Kitzen, J. M., Pergolizzi, J. V., Jr, Taylor, R., Jr, & Raffa, R. B. (2018). Crisaborole and apremilast: PDE4 inhibitors with similar mechanism of action, different indications for management of inflammatory skin conditions. *Pharmacology & Pharmacy, 9*(09), 357.

Ko, W.-C., Shih, C.-M., Lai, Y.-H., Chen, J.-H., & Huang, H.-L. (2004). Inhibitory effects of flavonoids on phosphodiesterase isozymes from guinea pig and their structure–activity relationships. *Biochemical Pharmacology, 68*(10), 2087–2094.

Li, S., Wang, R., Hu, X., Li, C., & Wang, L. (2021). Bio-affinity ultra-filtration combined with HPLC-ESI-qTOF-MS/MS for screening potential α-glucosidase inhibitors from Cerasus humilis (Bge.) Sok. leaf-tea and in silico analysis. *Food Chemistry, 131528*. https://doi.org/10.1016/j.foodchem.2021.131528

Li, S., Wang, R., Hu, X., Li, C., & Wang, L. (2022). Bio-affinity ultra-filtration combined with HPLC-ESI-qTOF-MS/MS for screening potential α-glucosidase inhibitors from Cerasus humilis (Bge.) Sok. leaf-tea and in silico analysis. *Food Chemistry, 373*, Article 131528.

Li, Song, J., Qiao, C., Zhou, Y., Qian, K., Lee, K., & Xu, H. (2010). A novel strategy to rapidly explore potential chemical markers for the discrimination between raw and processed Radix Rehmanniae by UHPLC–TOFMS with multivariate statistical analysis. *Journal of Pharmaceutical and Biomedical Analysis, 51*(4), 812–823.

Li, Y., Liu, X., Zhao, D., Liao, Y., Zhang, L., Zhang, F., … Cui, Z. (2018). Tetrahydroquinoline and tetrahydroisoquinoline derivatives as potential selective PDE4B inhibitors. *Bioorganic & Medicinal Chemistry Letters, 28*(19), 3271–3275.

Li, Z., Cai, Y.-H., Cheng, Y.-K., Lu, X., Shao, Y.-X., Li, X., … Luo, H.-B. (2013). Identification of novel phosphodiesterase-4D inhibitors prescreened by molecular dynamics-augmented modeling and validated by bioassay. *Journal of Chemical Information and Modeling, 53*(4), 972–981.

Ma, X., Wu, Y., Li, Y., Huang, Y., Liu, Y., Luo, P., & Zhang, Z. (2020). Rapid discrimination of Notopterygium incisum and Notopterygium franchetii based on characteristic compound profiles detected by UHPLC-QTOF-MS/MS coupled with multivariate analysis. *Phytochemical Analysis, 31*(3), 355–365.

Morris, G. M., Goodsell, D. S., Halliday, R. S., Huey, R., Hart, W. E., Belew, R. K., & Olson, A. J. (1998). Automated docking using a Lamarckian genetic algorithm and an empirical binding free energy function. *Journal of Computational Chemistry, 19*(14), 1639–1662.

Purushothaman, B., Arumugam, P., & Song, J. M. (2018). A novel catecholopyrimidine based small molecule PDE4B inhibitor suppresses inflammatory cytokines in atopic mice. *Frontiers in Pharmacology, 9*, 485.

Roy, S., Nandi, R. K., Ganai, S., Majumdar, K. C., & Das, T. K. (2017). Binding interaction of phosphorus heterocycles with bovine serum albumin: A biochemical study. *Journal of Pharmaceutical Analysis, 7*(1), 19–26.

Shu, J., Li, L., Zhou, M., Yu, J., Peng, C., Shao, F., … Huang, H. (2018). Three new flavonoid glycosides from Smilax glabra and their anti-inflammatory activity. *Natural Product Research, 32*(15), 1760–1768.

Su, X., Wu, Y., Li, Y., Huang, Y., Liu, Y., Luo, P., & Zhang, Z. (2019). Effect of different post-harvest processing methods on the chemical constituents of Notopterygium franchetii by an UHPLC-QTOF-MS-MS Metabolomics Approach. *Molecules, 24*(17), 3188.

Thabrew, M. I., Mitry, R. R., Morsy, M. A., & Hughes, R. D. (2005). Cytotoxic effects of a decoction of Nigella sativa, Hemidesmus indicus and Smilax glabra on human hepatoma HepG2 cells. *Life Sciences, 77*(12), 1319–1330.

Wang, S., Huai, J., Shang, Y., Xie, L., Cao, X., Liao, J., … Dai, R. (2020). Screening for natural inhibitors of 5-lipoxygenase from Zi-shen pill extract by affinity ultrafiltration coupled with ultra performance liquid chromatography-mass spectrometry. *Journal of Ethnopharmacology, 254*, Article 112733.

Worley, B., & Powers, R. (2016). PCA as a practical indicator of OPLS-DA model reliability. *Current Metabolomics, 4*(2), 97–103.

Wu, Y., Zhang, Z., Chen, T., Cheng, C., Zhang, Z., Zhou, H., & Luo, P. (2020). Comparison of two Polygonum chinense varieties used in Chinese cool tea in terms of chemical profiles and antioxidant/anti-inflammatory activities. *Food Chemistry, 310*, Article 125840.

Xie, X., Chen, C., & Fu, X. (2021). Screening α-glucosidase inhibitors from four edible brown seaweed extracts by ultra-filtration and molecular docking. *LWT, 138*, Article 110654.

Xu, S., Shang, M.-Y., Liu, G.-X., Xu, F., Wang, X., Shou, C.-C., & Cai, S.-Q. (2013). Chemical constituents from the rhizomes of Smilax glabra and their antimicrobial activity. *Molecules, 18*(5), 5265–5287.

Zhang, Q.-F., Zhang, Z.-R., & Cheung, H.-Y. (2009). Antioxidant activity of Rhizoma Smilacis Glabrae extracts and its key constituent-astilbin. *Food Chemistry, 115*(1), 297–303.

Zhang, X., Dong, G., Li, H., Chen, W., Li, J., Feng, C., … Li, M. (2019). Structure-aided identification and optimization of tetrahydro-isoquinolines as novel PDE4 inhibitors leading to discovery of an effective antipsoriasis agent. *Journal of Medicinal Chemistry, 62*(11), 5579–5593.

Zheng, D., Zhang, L., & Zhang, Q.-F. (2018). Isomerization of astilbin and its application for preparation of the four stereoisomers from Rhizoma Smilacis Glabrae. *Journal of Pharmaceutical and Biomedical Analysis, 155*, 202–209.